Enhanced antioxidative properties of carbon-coated W-doped NiMoN catalysts for robust water electrolysis under fluctuating electricity

Supporting Information

1. Characterizations

Scanning electron microscopy (SEM) and energy-dispersive X-ray spectroscopy (EDX) elemental mapping were conducted using a Zeiss SUPRA 55 electron microscope. Examinations of High-resolution transmission electron microscopy (HRTEM) and high-angle annular dark field - scanning transmission electron microscopy (HAADF-STEM) was conducted using a JEOL JEM-2100F. X-ray diffraction (XRD) patterns were recorded on a Bruker D8-Advance diffractometer using Cu Kα radiation (hυ = 1486.6 eV) with a scan rate of 5° per minute. Raman spectra were acquired using a Renishaw inVia Reflex with a 514 nm laser. X-ray photoelectron spectroscopy (XPS) measurements were conducted on an ESCALAB 250Xi equipped with a monochromated Al Kα 150 W X-ray source.

2. Electrochemical Measurements

Electrochemical measurements were performed on an electrochemical workstation (CS 150, Wuhan Corrtest Instruments Co., Ltd.) using a three-electrode system. The prepared electrodes (1×1 cm^2) served as the working electrode, while a graphite electrode and a saturated calomel electrode (SCE) acted as the counter and reference electrodes, respectively. Prior to measurement, the 1 M KOH electrolyte was purged with Ar for 30 minutes to eliminate dissolved gases. In 1 M KOH, the potential vs. reversible hydrogen electrode (RHE) was calculated as E(RHE) = E(SCE) + 0.2415 + 0.05916 * pH (for 1 M KOH). All measurements were conducted without iR compensation, and the electrolyte resistance was approximately 0.6 Ω.

Linear sweep voltammetry (LSV) tests were conducted at a scan rate of 1 mV s^{-1}. Tafel plots were derived from the LSV data. Tafel curves were measured using the workstation over a potential range of -1.05 to -1.2 V (vs. SCE) at a scan rate of 1 mV s^{-1}. Electrochemical impedance spectroscopy (EIS) spectra were recorded at an overpotential of -0.05 V (vs. RHE), superimposing signals in a frequency range of 100,000 to 0.05 Hz with an amplitude of 5 mV. The double-layer capacitance (C_{dl}), proportional to the electrochemically active surface area (ECSA) was determined through cyclic voltammetry (CV) tests in a scan rate range from 2 to 10 mV s^{-1}. Multi-current step (ISTEP) tests were performed at -10, -100, -300, -500, -800, and -1000 mA cm^{-2} ， increasing step by step in sequence with each step taking 300 seconds.

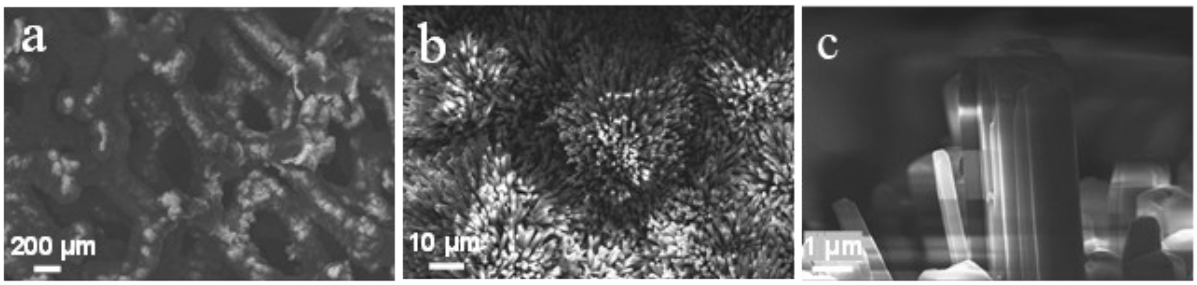

Figure S1. SEM images of NiMoWO.

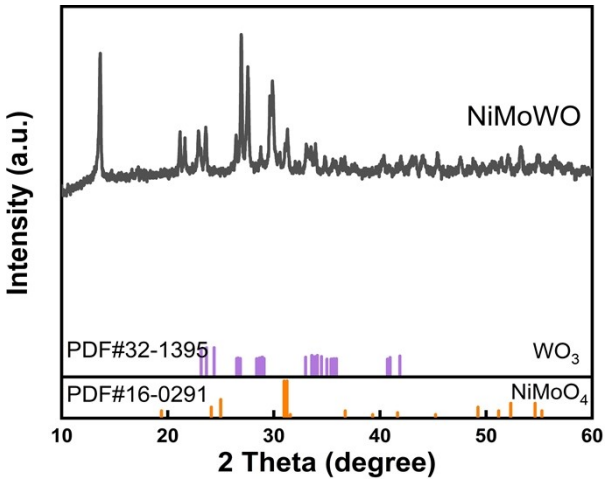

Figure S2. XRD patterns of NiMoWO.

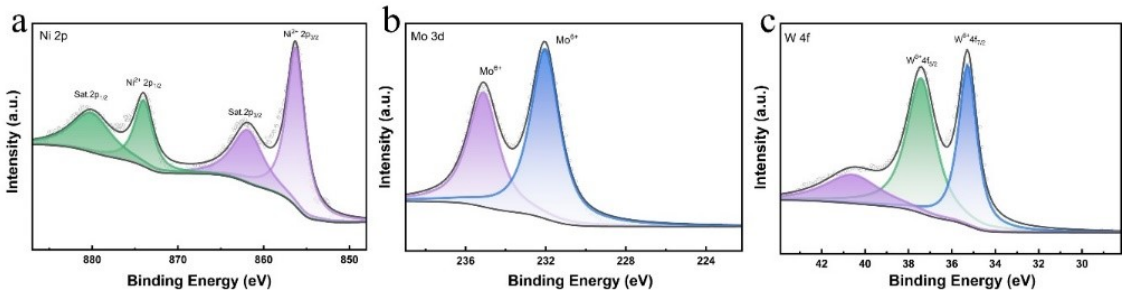

Figure S3. XPS results of NiMoWO.

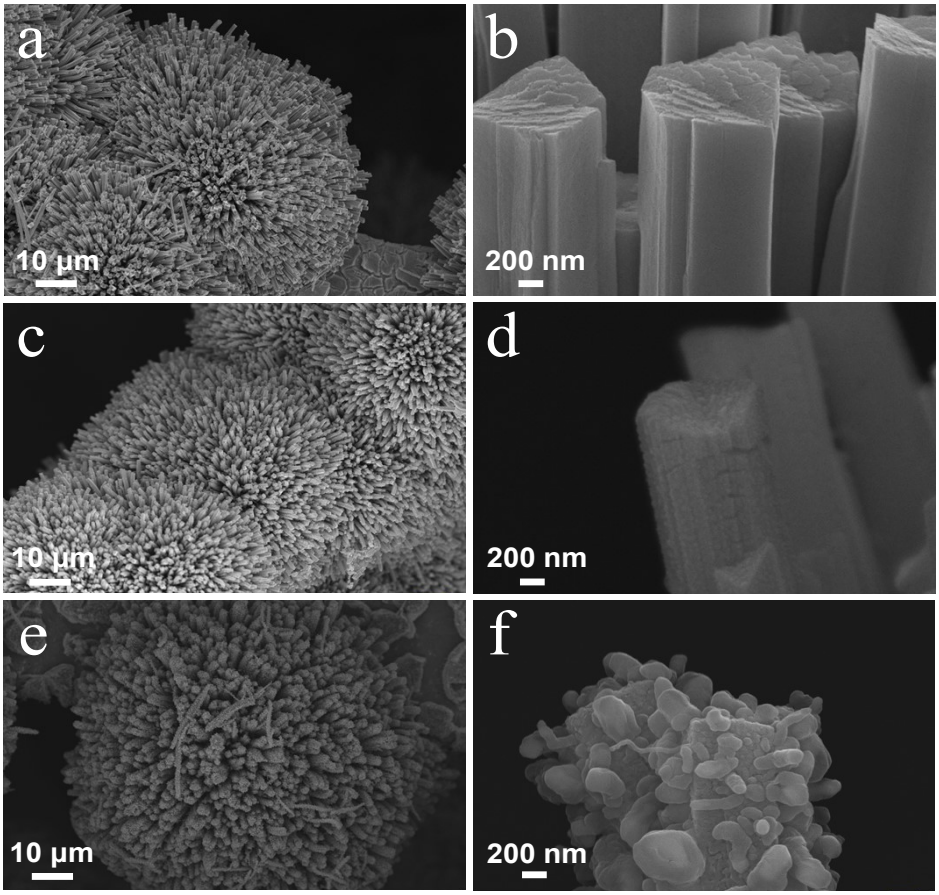

Figure S4. SEM images of W-NiMoN@NC at various heat treatment temperature: (a-b) 500℃, (c-d) 600℃, (e-f) 700℃.

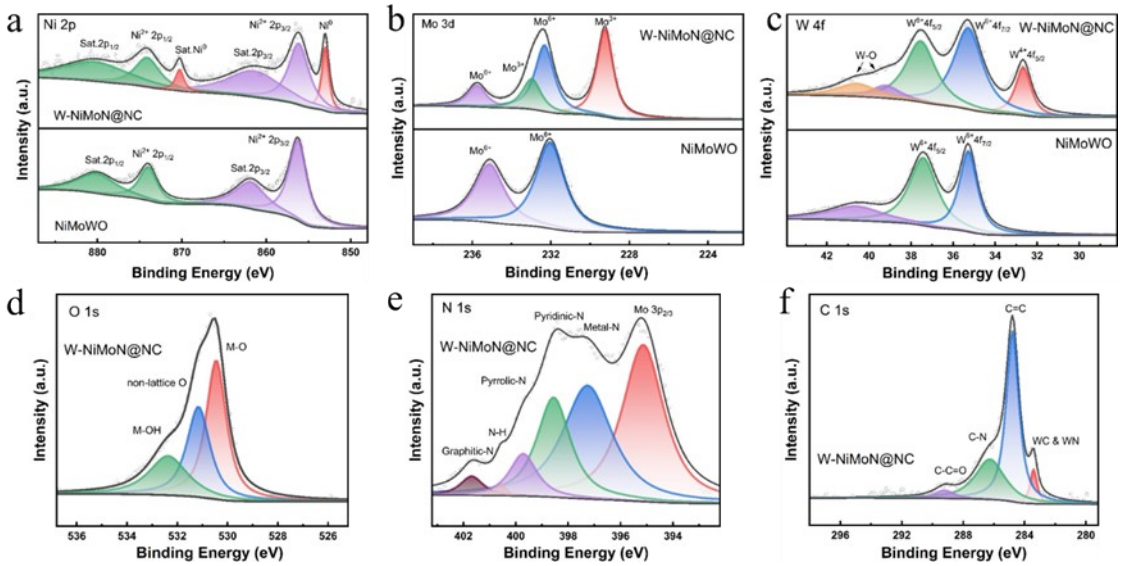

Figure S5. XPS results of W-NiMoN@NC and NiMoWO: (a) Ni 2p; (b) Mo 3d; (c) W 4f; (d) O 1s; (e) N 1s; (f) C 1s.

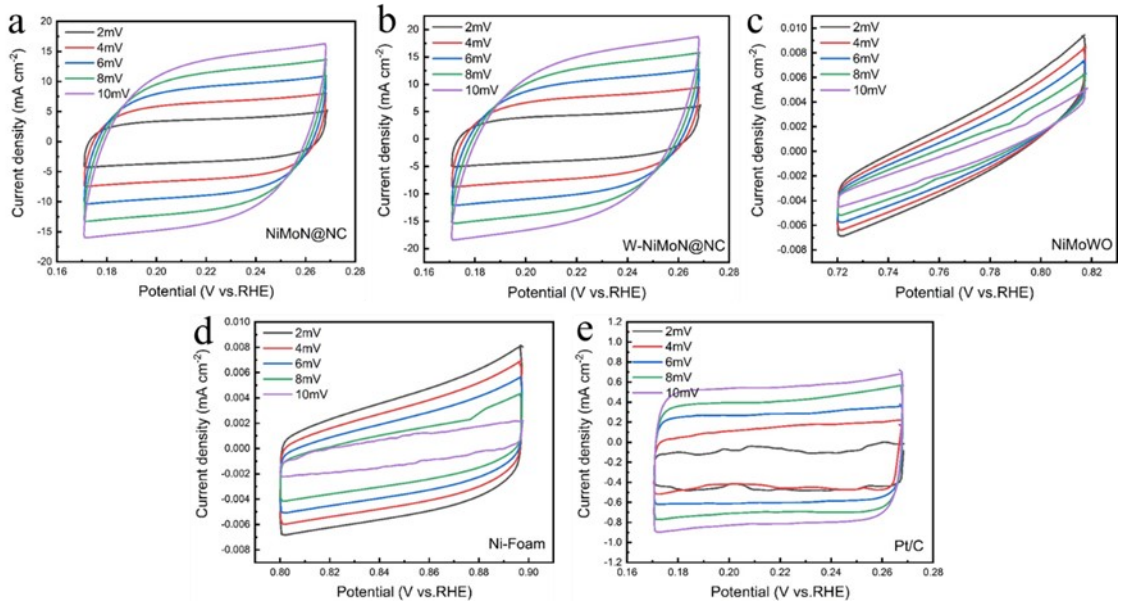

Figure S6. Cyclic voltammetry curves of W-NiMoN@NC, NiMoN@NC, W-doped $NiMoO_4$, Ni-Foam and Pt/C.

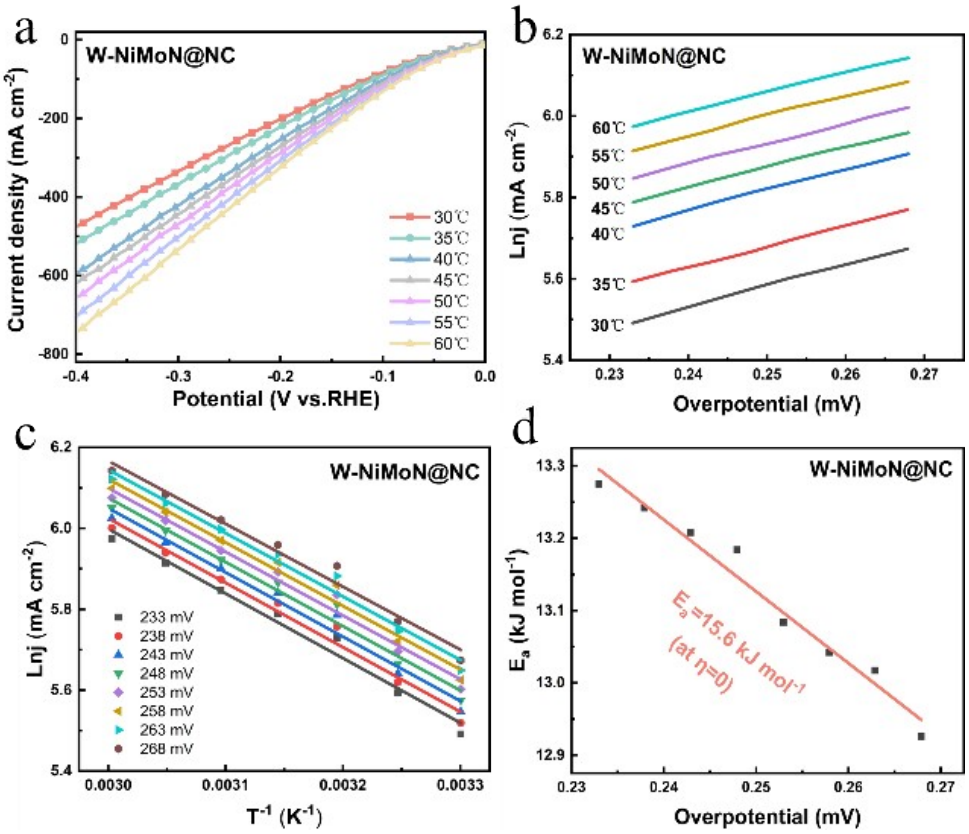

Figure S7. Arrhenius equation test diagram of W-NiMoN@NC.

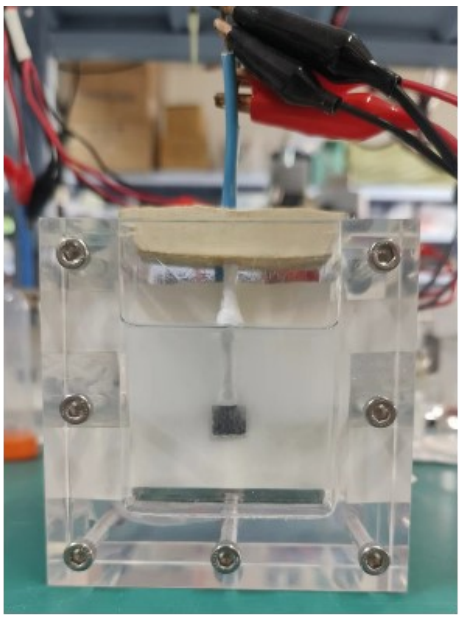

Figure S8. Device diagram of cyclic electrolysis test.

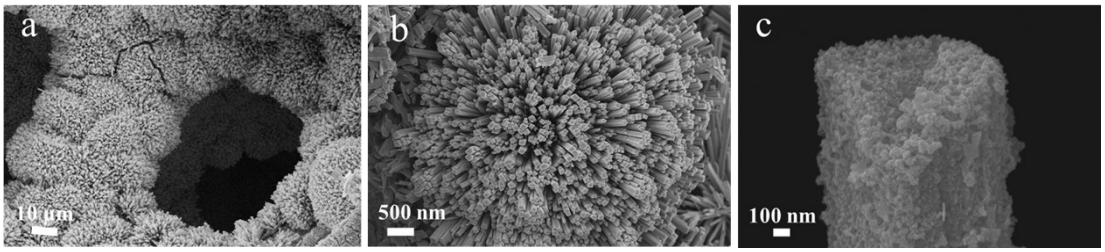

Figure S9. (a-c) SEM images of W-NiMoN@NC after fluctuating electrolysis.

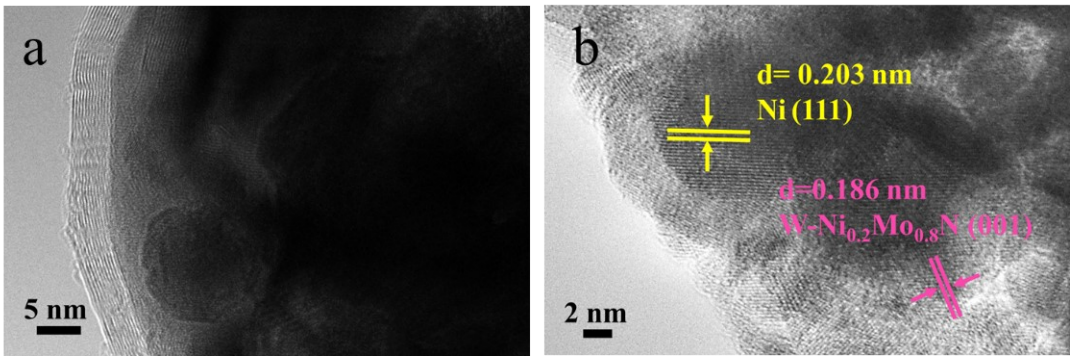

Figure S10. (a-b) HRTEM images of W-NiMoN@NC after fluctuating electrolysis.

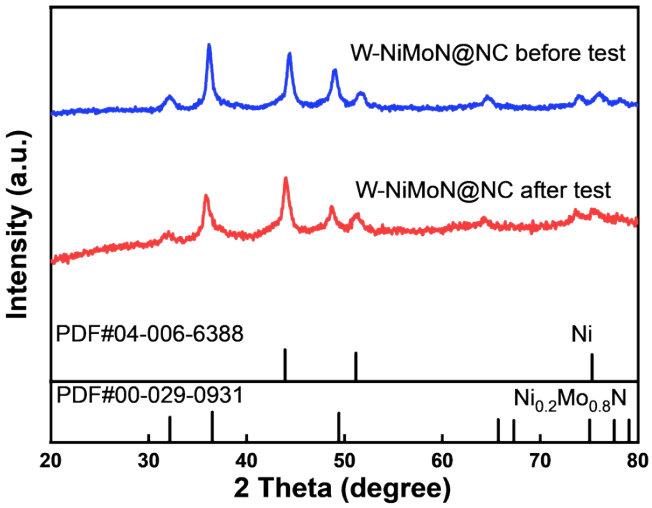

Figure S11. XRD results before and after fluctuating electrolysis of W-NiMoN@NC.

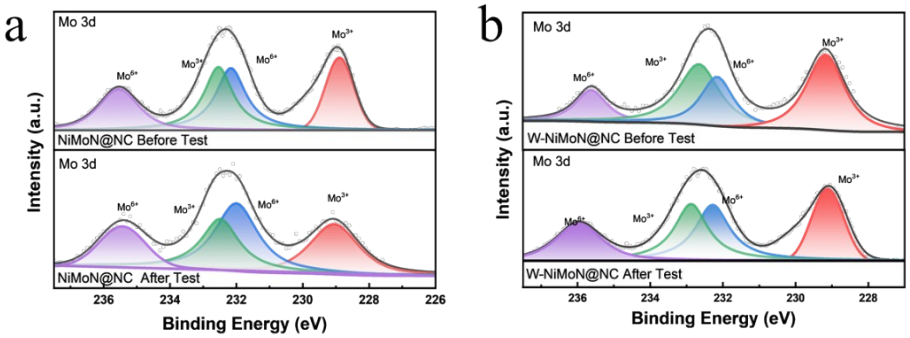

Figure S12. XPS results before and after fluctuating electrolysis: (a) Mo 3d of NiMoN@NC, (b) Mo 3d of W-NiMoN@NC.

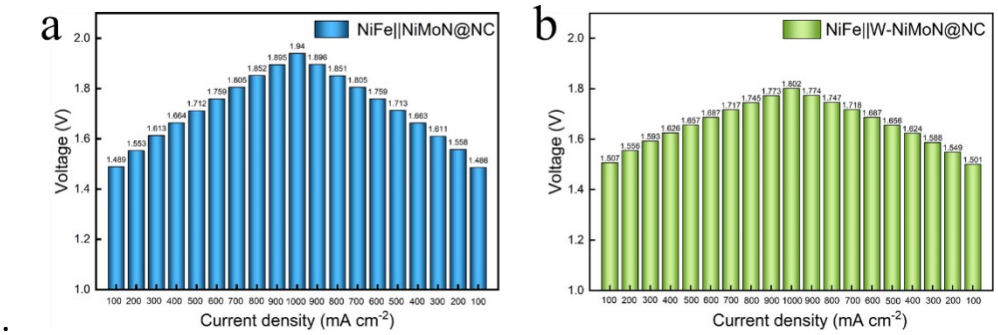

Figure S13. (a-b) The bar diagram of the Overall water splitting in different current density in 27 ℃,30% KOH for NiFe(+)||NiMoN@NC and NiFe(+)||W-NiMoN@NC.

Table S1. Summary of evolved gases from DCDA

Sample	Major Pyrolysis Temperature	Evolved Gas Species
DCDA	200 ~ 400℃	Hydrogen, Ammonia, Water Vapor, Cyanide-containing gases
	600 ~ 800℃	Ammonia, Primary Amines, Cyanide-containing gases, Carbon Dioxide, Pyridine Nitrogen-containing Heterocyclic gases

Table S2 Comparison of HER activity of W-NiMoN@NC electrode with recently reported Ni-based catalysts in 1.0 M KOH.

Catalysts	**η 10 (mV vs RHE)**	**η 100 (mV vs RHE)**	**Ref.**
W-NiMoN@NC	**13**	**67**	**This work**
Ni_{SA}-O/Mo_2C	133	-	[1]
Ni-Fe-Sn	27	-	[2]
$Ni_6Fe_1Mo_1$-LDH/NF	104	-	[3]

SeNi(Fe)OOH	22	-	[4]
A-NiMoO-P	-	65	[5]
Pt-NiMo-OH/NF	34	-	[6]
$NiSe/Ni_3Se_2$-Fe	144	-	[7]
$NF/NiMoO-H_2$	11	-	[8]
NiFeMo	180	-	[9]
Fe-Ni@NC-CNTs	202	-	[10]
NiCoP@NiMn LDH/NF	-	116	[11]
Ni@NCNT/NiMoN/NF	15	-	[12]
$MoNi_4/MoO_2$@Ni	15	-	[13]
$(Ni–MoO_2)$@C	50	-	[14]
$Ni_{0.33}Mo_{0.67}$-900	37	-	[15]
NiFeO/NiMo	46	-	[16]

[1] Hou M, Zheng L, Zhao D, Tan X, Feng W, Fu J, et al. Microenvironment reconstitution of highly active Ni single atoms on oxygen-incorporated Mo2C for water splitting. Nat Commun. 2024;15. DOI: 10.1038/s41467-024-45533-3.

[2] You S, Wu Y, Wang Y, He Z, Yin L, Zhang Y, et al. Pulse-electrodeposited Ni–Fe–Sn films supported on Ni foam as an excellent bifunctional electrocatalyst for overall water splitting. Int J Hydrogen Energy. 2022;47:29315-26. DOI: 10.1016/j.ijhydene.2022.06.265.

[3] Guo J, Wang K, Zhang H, Zhang H. Enhanced Electrocatalytic Activity of Mo-Doped NiFe Layered Double Hydroxide Nanosheet Arrays for the Hydrogen Evolution Reaction. ACS Applied Nano Materials. 2022;6:379-89. DOI: 10.1021/acsanm.2c04519.

[4] Li Q, Chen B, Huang L, Zhu S, Qian Y, Wu D, et al. S-doped Ni(Fe)OOH bifunctional electrocatalysts for overall water splitting. Int J Hydrogen Energy. 2024;51:1392-406. DOI: 10.1016/j.ijhydene.2023.07.291.

[5] Li Q, Chen C, Luo W, Yu X, Chang Z, Kong F, et al. In Situ Active Site Refreshing of Electro-Catalytic Materials for Ultra-Durable Hydrogen Evolution at Elevated Current Density. Adv Energy Mater. 2024;14. DOI: 10.1002/aenm.202304099.

[6] Zhang X, Han Y, Cai W, Zhang D, Wang Z, Li H, et al. Platinum Clusters Anchored Amorphous NiMo Hydroxide with Collaborative Electronic Transfer for Overall Water Splitting under High Current Density. Advanced Materials Interfaces. 2022;9. DOI: 10.1002/admi.202102154.

[7] Deng R, Yao H, Wang Y, Wang C, Zhang S, Guo S, et al. Interface effect of Fe doped

NiSe/Ni3Se2 heterojunction as highly efficient electrocatalysts for overall water splitting. Chem Eng J. 2024;488. DOI: 10.1016/j.cej.2024.150996.

[8] Yu Z-Y, Lang C-C, Gao M-R, Chen Y, Fu Q-Q, Duan Y, et al. Ni–Mo–O nanorod-derived composite catalysts for efficient alkaline water-to-hydrogen conversion via urea electrolysis. Energy Environ Sci. 2018;11:1890-7. DOI: 10.1039/c8ee00521d.

[9] Wang Z, Chen H, Bao J, Song Y, She X, Lv G, et al. Amorphized core–shell NiFeMo electrode for efficient bifunctional water splitting. Appl Surf Sci. 2023;607. DOI: 10.1016/j.apsusc.2022.154803.

[10] Zhao X, Pachfule P, Li S, Simke JRJ, Schmidt J, Thomas A. Bifunctional Electrocatalysts for Overall Water Splitting from an Iron/Nickel-Based Bimetallic Metal–Organic Framework/Dicyandiamide Composite. Angewandte Chemie International Edition. 2018;57:8921-6. DOI: 10.1002/anie.201803136.

[11] Wang P, Qi J, Chen X, Li C, Li W, Wang T, et al. Three-Dimensional Heterostructured NiCoP@NiMn-Layered Double Hydroxide Arrays Supported on Ni Foam as a Bifunctional Electrocatalyst for Overall Water Splitting. ACS Appl Mater Interfaces. 2019;12:4385-95. DOI: 10.1021/acsami.9b15208.

[12] Gong Y, Wang L, Xiong H, Shao M, Xu L, Xie A, et al. 3D self-supported Ni nanoparticle@N-doped carbon nanotubes anchored on NiMoN pillars for the hydrogen evolution reaction with high activity and anti-oxidation ability. J Mater Chem A. 2019;7:13671-8. DOI: 10.1039/c9ta03473k.

[13] Zhang J, Wang T, Liu P, Liao Z, Liu S, Zhuang X, et al. Efficient hydrogen production on MoNi4 electrocatalysts with fast water dissociation kinetics. Nat Commun. 2017;8:15437. DOI: 10.1038/ncomms15437.

[14] Qian G, Chen J, Luo L, Yu T, Wang Y, Jiang W, et al. Industrially Promising Nanowire Heterostructure Catalyst for Enhancing Overall Water Splitting at Large Current Density. ACS Sustainable Chem Eng. 2020;8:12063-71. DOI: 10.1021/acssuschemeng.0c03263.

[15] Shang P, Ye Z, Ding Y, Zhu Z, Peng X, Ma G, et al. Nanosponge-like Solid Solution of NiMo with a High Hydrogen Evolution Reaction Performance over a Wide Range of Current Densities. ACS Sustainable Chem Eng. 2020. DOI: 10.1021/acssuschemeng.0c00783.

[16] Shen Y, Wu P, Wang C, Yuan W, Yang W, Shang X. Electrodeposition of amorphous Ni–Fe–Mo composite as a binder-free and high-performance electrocatalyst for hydrogen generation from alkaline water electrolysis. Int J Hydrogen Energy. 2023;48:33130-8. DOI: 10.1016/j.ijhydene.2023.03.327.